iconducting behavior of the compound.

Acknowledgment. We thank the donors of the Petroleum Research Fund, administered by the American Chemical Society, for partial support of this research. We also gratefully acknowledge the support of the National Science Foundation for support through a Presidential Young Investigator Award (Grant DMR-8858151) and the Robert A. Welch Foundation for support through Grant A-1132. We thank Dr. Nancy McGuire and Roberta Peascoe for assistance in structure refinement and Prof. Abraham Clearfield for generous use of his facilities. Lisa Donaghe performed the microprobe analyses.

Appendix

The extended Hückel method was used for all band structure calculations; parameters appear in Table IV. Valence-state ionization energies (H_{ii}'s) for Ta were previously obtained from a charge-iterative calculation on $Ta_9S_6Ni_2$.[27] Other parameters have been cited previously.[28-30] Except for the Ta_6S_5 model calculation, structural parameters were taken from crystallographic data. For Ta_6S_5, geometric parameters were chosen to closely approximate the chain structure imbedded in Ta_3S_2.

Band structure calculations were carried out by using *k* point meshes as follows: Ta metal, 32 *k* points (primitive bcc lattice); Ta_2S, 32 *k* points for the 36-atom orthorhombic cell; Ta_3S_2, 30 *k* points for the primitive (20-atom) cell; Ta_6S_5, 25 *k* points for the one-dimensional $(Ta_{12}S_{10})S_{10}$ unit cell. Each of these *k* point meshes refers to the number of points used in the irreducible wedge of the appropriate Brillouin zones. All DOS curves were smoothed with Gaussian functions with a standard half-width of 0.05 eV.

Supplementary Material Available: For Ta_3S_2, a table of anisotropic thermal parameters (1 page); a table of structure factors (7 pages). Ordering information is given on any current masthead page.

---

[27] Hughbanks, T. Unpublished research.

[28] Basch, H.; Gray, H. B. *Theor. Chim. Acta* **1966**, *4*, 367.

[29] Baranovskii, V. I.; Nikolskii, A. B. *Teor. Eksp. Khim.* **1967**, *3*, 527.

[30] Clementi, E.; Roetti, C. *At. Nucl. Data Tables* **1974**, *14*, 177.

Contribution from the Laboratoire de Chimie Inorganique, URA No. 420, Université de Paris Sud,
91405 Orsay, France, Department of Chemistry, University of Bergen, 5007 Bergen, Norway,
and Laboratoire de Chimie des Métaux de Transition, URA No. 419,
Université Pierre et Marie Curie, 75232 Paris, France

Structural and Magnetic Versatility of the Mn(II)/$[Cu(X_4obbz)]^{2-}$ System (X_4obbz = Oxamido-*N*,*N'*-bis(3,5-dihalogenobenzoato; X = Cl, Br). Crystal Structures and Magnetic Properties of $MnCu(Cl_4obbz)(H_2O)_5$ and $MnCu(Br_4obbz)(H_2O)_3·2.5H_2O$

Keitaro Nakatani,[1a] Jorunn Sletten,[1b] Sabine Halut-Desporte,[1c] Suzanne Jeannin,[1c] Yves Jeannin,[1c] and Olivier Kahn*,[1a]

Received April 23, 1990

The two compounds $MnCu(Cl_4obbz)(H_2O)_5$ (**1**) and $MnCu(Br_4obbz)(H_2O)_3·2.5H_2O$ (**2**) have been synthesized. Cl_4obbz stands for oxamido-*N*,*N'*-bis(3,5-dichlorobenzoato) and Br_4obbz for oxamido-*N*,*N'*-bis(3,5-dibromobenzoato). Their crystal structures have been determined. The tetrachloro derivative crystallizes in the monoclinic system, space group $P2_1/n$, with a = 10.351 (4) Å, b = 19.130 (4) Å, c = 11.225 (2) Å, β = 97.82 (2)° with Z = 4 MnCu units. The structure consists of binuclear units with Mn(II) and Cu(II) ions bridged by a carboxylate group (Mn···Cu = 5.195 (1) Å). The bimetallic units are connected through Cu···Cl contacts of 2.930 and 3.422 Å. The configuration around the carboxylate bridge is of the anti–syn type. The tetrabromo derivative crystallizes in the monoclinic system, space group $P2_1/c$ with a = 9.294 (2) Å, b = 17.981 (4) Å, c = 15.021 (2) Å, β = 100.00 (2)°, and Z = 4 MnCu units. The structure consists of alternating bimetallic chains with Mn(II) and Cu(II) ions bridged by oxamide (Mn···Cu = 5.341 (2) Å) and carboxylate (Mn···Cu = 5.394 (2) Å) groups. The chains are connected through Cu···Br contacts of 2.971 Å. The configuration around the carboxylate bridge is again of the anti–syn type. The magnetic properties of both compounds have been investigated in the 2–300 K temperature range. For **1**, the molar magnetic susceptibility χ_M follows the Curie law expected for uncoupled Mn(II) and Cu(II) ions. For **2**, χ_M varies as expected for a Mn(II)–Cu(II) pair with a quintet–septet energy gap equal to $3J = -87.0$ cm^{-1}. This rather strong antiferromagnetic interaction occurs through the oxamide bridge. For both compounds, the interaction through the carboxylate bridge is negligible owing to the anti–syn configuration around this bridge. The EPR spectra reveal long-range interactions not detectable through magnetic susceptibility measurements. The structural and magnetic differences between the two compounds are discussed.

Introduction

Recently, we described a molecular-based compound exhibiting a spontaneous magnetization and an hysteresis loop below T_c = 14 K. Its formula is $MnCu(obbz)·H_2O$ with obbz = oxamido-*N*,*N'*-bis(benzoato).[2,3] This compound was obtained from the reaction of the Mn(II) ion on the Cu(II) precursor $[Cu(obbz)]^{2-}$ schematized below:

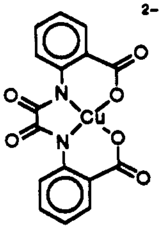

Actually, this reaction, in addition to $MnCu(obbz)·H_2O$, leads to another species of formula $MnCu(obbz)·5H_2O$, which shows

---

[1] (a) Université de Paris Sud. (b) University of Bergen. (c) Université Pierre et Marie Curie.

[2] Nakatani, K.; Carriat, J. Y.; Journaux, Y.; Kahn, O.; Lloret, F.; Renard, J. P.; Pei, Y.; Sletten, J.; Verdaguer, M. *J. Am. Chem. Soc.* **1989**, *111*, 5739.

[3] Kahn, O.; Pei, Y.; Nakatani, K.; Journaux, Y. *Mol. Cryst. Liq. Cryst.* **1989**, *176*, 481.

0020-1669/91/1330-0164$02.50/0 © 1991 American Chemical Society

a three-dimensional antiferromagnetic ordering at 2.3 K. MnCu(obbz)$\cdot H_2O$ and MnCu(obbz)$\cdot 5H_2O$ seem to have much the same structure, the four additional water molecules in the latter compound being noncoordinated to metal centers. The EXAFS and XANES spectra as well as the powder X-ray patterns are very similar and consistent with a structure of alternating bimetallic chains, the Mn(II) and Cu(II) ions being alternately bridged by the oxamide and the carboxylate groups. The magnetic behavior of MnCu(obbz)$\cdot 5H_2O$ substantiates this hypothesis. Indeed, it is characteristic of ferrimagnetic chain compounds with a minimum in the $\chi_M T$ versus T plot, χ_M being the molar magnetic susceptibility and T the temperature.[4-14] In spite of all these self-consistent data, the precise structure of MnCu(obbz)$\cdot H_2O$ remains unknown. All attempts to grow single crystals suitable for X-ray work have failed. Structural information concerning the exact coordination of the carboxylate bridge and of the packing of bimetallic chains within the crystal lattice would be of the utmost importance to understand the mechanism of the three-dimensional ferromagnetic ordering. Since we have not been able to obtain such information directly from MnCu(obbz)$\cdot H_2O$, we have decided to investigate other Mn(II)–Cu(II) system prepared from copper(II) precursors close to [Cu(obbz)]$^{2-}$. In this paper, we wish to report on the results obtained from the two new precursors [Cu(X_4obbz)]$^{2-}$ with X = Cl and Br, schematized below:

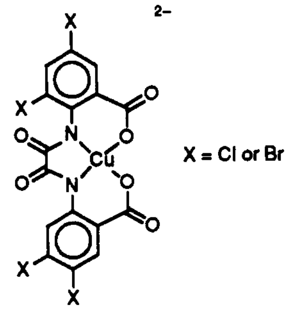

Cl_4obbz stands for oxamido-*N*,*N'*-bis(3,5-dibromobenzoato) and Br_4obbz for oxamido-*N*,*N'*-bis(3,5-dibromobenzoato). This work will bring witness of the magnificent versatility of this kind of chemistry. As a matter of fact, two new compounds have been synthesized with rather similar MnCu(Cl_4obbz)$(H_2O)_5$ (**1**) and MnCu(Br_4obbz)$(H_2O)_3\cdot 2.5H_2O$ (**2**) formulas. Their structures, however, are quite different. That of the tetrachloro derivative consists of binuclear units with Mn(II) and Cu(II) ions bridged by the carboxylate group. Apparently, the steric hindrance due to chlorine substituents in the 3-position prevents the coordination of the oxamide group on the Mn(II) ion. On the other hand, the structure of the tetrabromo derivative is that of bimetallic alternating chains. Although the atomic radius of the bromine atom is larger than that of the chlorine atom (1.14 and 0.99 Å, respectively), the coordination of the oxamide group on the manganese atom occurs thanks to a pronounced bending of the Mn–oxamide–Cu network.

Table I: Crystallographic Data for MnCu(Cl_4obbz)$(H_2O)_5$ (**1**) and MnCu(Br_4obbz)$(H_2O)_3\cdot 2.5H_2O$ (**2**)

	1	**2**
chem formula	$CuMnC_{16}H_{14}N_2O_{11}Cl_4$	$CuMnC_{16}H_{15}N_2O_{11.5}Br_4$
a, Å	10.351 (4)	9.295 (2)
b, Å	19.130 (4)	17.981 (4)
c, Å	11.225 (2)	15.021 (2)
β, deg	97.82 (2)	100.00 (2)
V, Å^3	2202 (2)	2472 (1)
Z	4	4
fw	670.59	857.40
space group	$P2_1/n$ (No. 14)	$P2_1/c$ (No. 14)
T, K	294	294
λ, Å	0.71069	0.71069
ρ(calcd), g cm^{-3}	2.023	2.30
μ, cm^{-1}	20.72	78.2
transm coeff	0.72–1.27	
abs cor		DIFABS[a]
$R(F_o)$	0.043	0.0345
$R_w(F_o)$	0.040	0.0390

[a] Walker, N., Stuart, D. *Acta Crystallogr., Sect. A* **1983**, *A34*, 159.

The paper is organized as follows: The syntheses, structures, and magnetic properties of the two compounds **1** and **2** will be successively described, and then the information arising from this work and concerning the chemistry and the physics of this class of bimetallic compounds will be summed up and discussed.

Experimental Section

Materials. 2-Amino-3,5-dichlorobenzoic and 2-amino-3,5-dibromobenzoic acids were purchased from Lancaster, oxalyl chloride was purchased from Janssen, copper(II) nitrate was purchased from Aldrich, and manganese(II) perchlorate was purchased from Fluka, and all were used as received. The chemical analyses were performed by the Laboratoire Central de Microanalyses du CNRS.

Syntheses. Both **1** and **2** were prepared in three steps, namely the synthesis of the ligand $H_4(X_4obbz)\cdot nH_2O$, then that of the sodium salt of the copper(II) precursor Na_2[Cu(X_4obbz)]$\cdot nH_2O$, and finally that of the Mn(II)–Cu(II) compound.

MnCu(Cl_4obbz)$(H_2O)_5$ (1). To a solution of 4.1 g (20 × 10^{-3} mol) of 2-amino-3,5-dichlorobenzoic acid in 20 mL of THF was added dropwise 1.4 g (11 × 10^{-3} mol) of oxalyl chloride. The mixture was stirred and gently heated up to 50 °C for about 2 h. The ligand $H_4(X_4obbz)\cdot 1.5H_2O$ separated as a white-gray powder from the cooled solution after adding 100 mL of diethyl ether. It was then filtered, washed with diethyl ether and water, and dried under vacuum. The yield was about 50%. Anal. Calcd for $C_{16}H_{11}N_2O_{7.5}Cl_4$: C, 38.95; H, 2.23; N, 5.68; O, 24.34; Cl, 28.80. Found: C, 39.38; H, 2.39; N, 5.31; O, 24.11; Cl, 28.69. Then 2.5 g (5 × 10^{-3} mol) of this ligand were dissolved in 100 mL of an aqueous solution containing 0.8 g (20 × 10^{-3} mol) of NaOH. A 50-mL aliquot of an aqueous solution containing 1.2 g (5 × 10^{-3} mol) of $Cu(NO_3)_2\cdot 3H_2O$ was added under constant stirring. The resulting blue-green solution was then filtered and allowed to evaporate slowly almost to dryness. Absolute ethanol was added, and the sodium salt of the copper(II) precursor precipitated as a dark violet polycrystalline powder. It was filtered, washed with cold absolute ethanol, and dried. The chemical analysis revealed that the copper(II) precursor was not pure but contained some $NaNO_3$. This is due to the fact that both compounds are very soluble in water and, therefore, difficult to separate. The atomic ratio C/Cu, however, was equal to 16/1, as expected for Na_2[Cu(Cl_4obbz)]$\cdot nH_2O$. Finally, single crystals of MnCu(Cl_4obbz)$(H_2O)_5$ were obtained by slow diffusion in a H-shaped tube of two solutions, one containing 57 mg (10^{-4} mol) of Na_2[Cu(Cl_4obbz)]$\cdot nH_2O$ dissolved in a 4/1 water–ethanol mixture and the other one containing 36 mg (10^{-4} mol) of manganese(II) perchlorate dissolved in the same mixture. The process took about 3 months. Anal. Calcd for $C_{16}H_{14}N_2O_{11}Cl_4CuMn$ (**1**): C, 28.66; H, 2.10; N, 4.18; O, 26.24; Cl, 21.15; Cu, 9.48; Mn, 8.19. Found: C, 27.99; H, 2.48; N, 3.98; O, 25.50; Cl, 20.87; Cu, 9.80; Mn, 7.82.

MnCu(Br_4obbz)$(H_2O)_3\cdot 2.5H_2O$ (2). The synthesis was very similar to that of the tetrachloro derivative, the 2-amino-3,5-dibromobenzoic acid being used instead of the 2-amino-3,5-dichlorobenzoic acid as starting material. The main difference between the two preparations was the conditions of the final slow diffusion. In the present case, the copper(II) precursor and manganese(II) perchlorate were dissolved in a 4/1

---

(4) Verdaguer, M.; Julve, M.; Michalowicz, A.; Kahn, O. *Inorg. Chem.* **1983**, *22*, 2624.
(5) Drillon, M.; Gianduzzo, J. C.; Georges, R. *Phys. Lett.* **1983**, *96A*, 413.
(6) Gleizes, A.; Verdaguer, M. *J. Am. Chem. Soc.* **1984**, *106*, 3727.
(7) Verdaguer, M.; Gleizes, A.; Renard, J. P.; Seiden, J. *Phys. Rev.* **1984**, *B29*, 5144.
(8) Kahn, O. *Struct. Bonding (Berlin)* **1987**, *68*, 89. Kahn, O. In *Organic and Inorganic Low-Dimensional Crystalline Materials*; Delhaes, P., Drillon, M., Eds.; NATO ASI Series 168; Plenum: New York, 1987; p 93.
(9) Landee, C. P. In *Organic and Inorganic Low-Dimensional Crystalline Materials*; Delhaes, P., Drillon, M., Eds.; NATO ASI Series 168; Plenum: New York, 1987; p 75.
(10) Pei, Y.; Verdaguer, M.; Kahn, O.; Sletten, J.; Renard, J. P. *Inorg. Chem.* **1987**, *26*, 138.
(11) Kahn, O.; Pei, Y.; Verdaguer, M.; Renard, J. P.; Sletten, J. *J. Am. Chem. Soc.* **1988**, *110*, 782.
(12) Coronado, E.; Drillon, M.; Nugteren, P. R.; de Jongh, L. J.; Beltran, D. *J. Am. Chem. Soc.* **1988**, *110*, 3907.
(13) Coronado, E.; Drillon, M.; Nugteren, P. R.; de Jongh, L. J.; Beltran, D.; Georges, R. *J. Am. Chem. Soc.* **1989**, *111*, 3874.
(14) Drillon, M.; Coronado, E.; Georges, R.; Gianduzzo, J. C.; Curely, J. *Phys. Rev.* **1989**, *40*, 10992.

Table II. Atomic Parameters for Non-Hydrogen Atoms of $MnCu(Cl_4obbz)(H_2O)_5$[a]

atom	x/a	y/b	z/c	B_{eq}, Å^2
Cu	0.58010 (7)	0.24458 (5)	0.44528 (8)	1.50 (2)
Mn	0.259789 (9)	0.03429 (6)	0.3940 (1)	1.73 (2)
Cl(1)	0.8786 (2)	0.4326 (1)	0.3870 (2)	2.62 (4)
Cl(2)	1.1909 (1)	0.2537 (1)	0.1998 (2)	2.25 (4)
Cl(3)	0.3845 (2)	0.4542 (1)	0.5677 (2)	2.38 (4)
Cl(4)	−0.0320 (2)	0.3110 (1)	0.6602 (2)	2.73 (4)
O(1)	0.6347 (4)	0.3965 (3)	0.2318 (4)	2.2 (1)
O(2)	0.4018 (4)	0.4116 (2)	0.3147 (4)	2.0 (1)
O(3)	0.6928 (4)	0.1670 (2)	0.4322 (4)	2.0 (1)
O(4)	0.4472 (4)	0.1768 (2)	0.4696 (4)	2.0 (1)
O(5)	0.8418 (4)	0.1051 (3)	0.3601 (4)	2.4 (1)
O(6)	0.2433 (4)	0.1403 (2)	0.4408 (4)	1.8 (1)
O(7)	0.2871 (4)	−0.0760 (2)	0.3738 (4)	2.0 (1)
O(8)	0.4654 (4)	0.0465 (3)	0.3795 (5)	3.2 (1)
O(9)	0.0531 (4)	0.0143 (3)	0.3679 (5)	3.2 (1)
O(10)	0.2340 (5)	0.0467 (3)	0.1956 (5)	4.6 (1)
O(11)	0.2785 (4)	0.0153 (3)	0.5906 (4)	2.2 (1)
N(1)	0.6873 (4)	0.3099 (3)	0.3745 (5)	1.2 (1)
N(2)	0.4603 (4)	0.3211 (3)	0.4462 (5)	1.4 (1)
C(1)	0.6125 (6)	0.3593 (4)	0.3164 (6)	1.7 (2)
C(2)	0.4799 (6)	0.3670 (4)	0.3615 (6)	1.6 (2)
C(3)	0.8146 (5)	0.2964 (4)	0.3481 (6)	1.4 (1)
C(4)	0.9036 (6)	0.3493 (4)	0.3341 (6)	1.4 (1)
C(5)	1.0170 (6)	0.3372 (4)	0.2887 (6)	1.7 (2)
C(6)	1.0494 (5)	0.2701 (4)	0.2618 (6)	1.2 (1)
C(7)	0.9736 (6)	0.2156 (4)	0.2891 (6)	1.5 (1)
C(8)	0.8564 (5)	0.2268 (4)	0.3335 (6)	1.2 (1)
C(9)	0.7933 (5)	0.1630 (4)	0.3764 (6)	1.2 (1)
C(10)	0.3436 (5)	0.3190 (4)	0.4987 (6)	1.1 (1)
C(11)	0.2953 (6)	0.3774 (3)	0.5502 (6)	1.2 (1)
C(12)	0.1794 (6)	0.3761 (4)	0.5987 (6)	1.8 (2)
C(13)	0.1142 (6)	0.3140 (4)	0.5994 (6)	1.7 (2)
C(14)	0.1613 (5)	0.2536 (4)	0.5557 (6)	1.4 (1)
C(15)	0.2782 (5)	0.2560 (4)	0.5072 (5)	1.1 (1)
C(16)	0.3242 (6)	0.1868 (4)	0.4676 (6)	1.6 (1)

[a] For anisotropically refined atoms the isotropic equivalent thermal parameter is given as $B_{eq} = {}^4/_3\sum_i\sum_j\beta_{ij}\mathbf{a}_i\cdot\mathbf{a}_j$.

water–methanol mixture. Anal. Calcd for $C_{16}H_{15}N_2O_{11.5}Br_4CuMn$ (**2**): C, 22.41; H, 1.76; N, 3.27; O, 21.46; Br, 37.28; Cu, 7.41; Mn, 6.41. Found: C, 22.39; H, 1.53; N, 3.10; O, 21.92; Br, 35.89; Cu, 6.93; Mn, 5.96.

Crystallographic Data Collection and Structure Determination. All measurements were carried out at room temperature on Enraf-Nonius CAD4 diffractometer using graphite-monochromated Mo Kα radiation.

$MnCu(Cl_4obbz)(H_2O)_5$ (1). Details concerning conditions for crystallographic data collection and structure refinement are given in Table I. Cell dimensions were determined from 21 reflections with 2θ angles between 21 and 40°. Three reference reflections were monitored by repeating measurements every 2 h during data collection; no indication of crystal deterioration was observed. The usual correction for Lorentz and polarization effects was carried out. The structure was solved by direct methods. Mn, Cu, and the four Cl atoms were revealed in the *E* map, the remaining non-hydrogen atoms were located in two subsequent Fourier maps. Refinement was performed with the full-matrix least-squares method. After isotropic refinement, an empirical absorption correction was carried out,[15] the maximum and minimum correction coefficients for F_o obtained being 1.27 and 0.72, respectively. After anisotropic refinement, hydrogen atoms were located in a difference Fourier map. Hydrogen atoms bonded to carbon were refined with isotropic thermal parameters, while those bonded to water oxygen were kept fixed. The scattering curves with anomalous dispersion terms were those of Cromer and Waber.[16a] Atomic parameters for non-hydrogen atoms are given in Table II. Anisotropic thermal parameters for non-hydrogen atoms and coordinates for hydrogen atoms are listed in Tables SII and SIII, respectively. All calculations were carried out on a MICRO-Vax II computer with the Enraf-Nonius SDP-program.[16b]

$MnCu(Br_4obbz)(H_2O)_3{\cdot}2.5H_2O$ (2). Details concerning conditions for crystallographic data collection and structure refinement are given in Table I. Cell dimensions were determined from 25 reflections with 2θ angles between 24 and 28°. The structure was solved by direct methods (Cu, Mn, and Br atoms) followed by successive Fourier syntheses and least-squares refinements. Hydrogen atoms, except those of free water molecules, were located in difference Fourier maps. They were refined with overall isotropic thermal parameters, the values of which depended on the nature of the hydrogen. One value was used for the hydrogens of coordinated water molecules, and another one for hydrogens of aromatic rings. Atomic parameters for all atoms but hydrogens are given in Table III. Anisotropic thermal parameters for all atoms but hydrogens and coordinates for hydrogen atoms are listed in Tables SIV and SV, respectively.

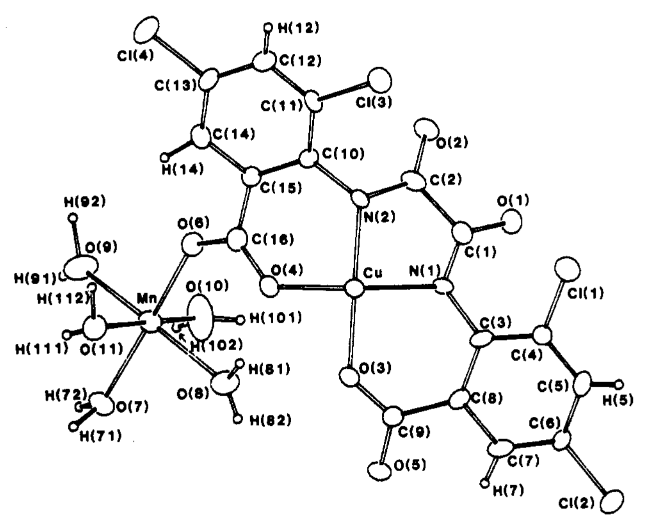

Figure 1. View of the $MnCu(Cl_4obbz)(H_2O)_5$ unit with atomic numbering scheme. Thermal ellipsoids are plotted at the 50% probability level.

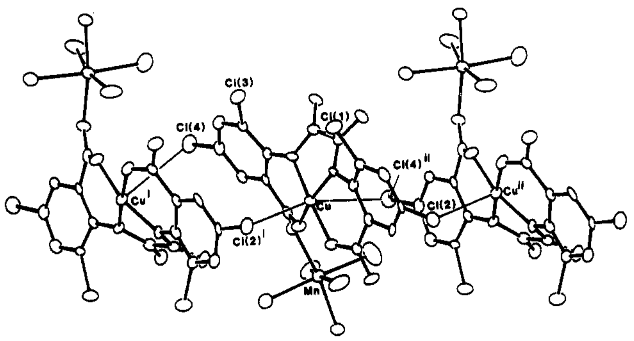

Figure 2. View of three molecules related by the *n*-glide symmetry operation. The Cu···Cl contacts are shown as single lines.

Magnetic Measurements. These were carried out with a Faraday-type magnetometer equipped with a helium continuous-flow cryostat in the 4–300 K temperature range and with a laboratory-made low-field SQUID magnetometer in the 2–20 K temperature range. $HgCo(NCS)_4$ was used as a susceptibility standard. Diamagnetic corrections were calculated as −382 × 10^{-6} cm^3 mol^{-1} and −426 × 10^{-6} cm^3 mol^{-1} from Pascal's constants for the tetrachloro and the tetrabromo derivatives, respectively.

EPR Spectra. The X-band powder EPR spectra were recorded at various temperatures between 4.2 and 300 K with a ER 200D Bruker spectrometer equipped with a helium continuous-flow cryostat, a Hall probe and a frequency meter.

Description of Structures

$MnCu(Cl_4obbz)(H_2O)_5$. Bond lengths and angles involving nonhydrogen atoms are listed in Tables IV and V. The structure consists of heterobinuclear molecules, as shown in Figure 1, a carboxylate group with the anti–syn configuration forming the bridge between Mn(II) and Cu(II) ions.

The manganese atom has somewhat distorted octahedral surroundings with five water molecules and one carboxylate oxygen atom in the coordination sphere. The copper atom is coordinated to two oxamide nitrogen and two carboxylate oxygen atoms in a slightly distorted square-planar arrangement. However, in the

---

(15) Walker, N.; Stuart, D. *Acta Crystallogr., Sect. A* **1983**, *A34*, 159.

(16) (a) Cromer, D. T.; Waber, J. T. In *International Tables For X-ray Crystallography*; Kynoch Press: Birmingham, England, 1974; Vol. IV, p 99, Table 2.2B. (b) Frenz, B. A. *The SDP-User's Guide, SDPVAX V.3*; Enraf-Nonius: Delft, The Netherlands, 1985.

Table III. Atomic and Thermal Parameters for Non-Hydrogen Atoms of MnCu(Br_4obbz)$(H_2O)_3\cdot2.5H_2O$

atom	x/a	y/b	z/c	U_{eq},[a] Å^2
Cu(1)	0.1540 (1)	−0.10860 (6)	−0.19779 (7)	0.0278
Br(1)	0.1440 (1)	−0.17689 (6)	0.11308 (7)	0.0423
Br(2)	−0.3582 (1)	−0.00555 (7)	0.10538 (8)	0.0471
Br(3)	0.5643 (1)	−0.23470 (8)	−0.02995 (8)	0.0533
Br(4)	0.8552 (1)	−0.21167 (7)	−0.32510 (8)	0.0486
Mn(1)	0.1381 (2)	−0.38106 (7)	−0.05825 (9)	0.0266
C(1)	0.105 (1)	−0.2223 (5)	−0.0920 (6)	0.0249
C(2)	0.236 (1)	−0.2452 (5)	−0.1360 (6)	0.0259
C(3)	−0.020 (1)	−0.1160 (5)	−0.0506 (6)	0.0230
C(4)	−0.122 (1)	−0.0649 (5)	−0.0945 (6)	0.0262
C(5)	−0.124 (1)	−0.0386 (5)	−0.1906 (6)	0.0239
C(6)	0.424 (1)	−0.1921 (5)	−0.2072 (6)	0.0223
C(7)	0.431 (1)	−0.1658 (5)	−0.2947 (6)	0.0248
C(8)	0.305 (1)	−0.1288 (5)	−0.3525 (6)	0.0293
C(9)	−0.016 (1)	−0.1272 (5)	0.0421 (6)	0.0298
C(10)	−0.115 (1)	−0.0961 (5)	0.0879 (7)	0.0306
C(11)	−0.222 (1)	−0.0489 (5)	0.0402 (7)	0.0273
C(12)	−0.225 (1)	−0.0319 (5)	−0.0480 (7)	0.0275
C(13)	0.556 (1)	−0.2163 (5)	−0.1545 (6)	0.0328
C(14)	0.682 (1)	−0.2210 (6)	−0.1893 (8)	0.0388
C(15)	0.683 (1)	−0.2005 (5)	−0.2764 (7)	0.0287
C(16)	0.559 (1)	−0.1709 (5)	−0.3287 (7)	0.0335
N(1)	0.0776 (8)	−0.1498 (4)	−0.0975 (5)	0.0241
N(2)	0.2935 (8)	−0.1890 (4)	−0.1735 (5)	0.0273
O(1)	0.0402 (7)	−0.2721 (3)	−0.0570 (4)	0.0311
O(2)	0.2741 (7)	−0.3121 (3)	−0.1322 (4)	0.0273
O(3)	−0.0067 (7)	−0.0404 (4)	−0.2247 (4)	0.0315
O(4)	0.2057 (7)	−0.0961 (4)	−0.3178 (4)	0.0354
O(5)	−0.2389 (7)	−0.0114 (4)	−0.2322 (5)	0.0401
O(6)	0.3019 (7)	−0.1286 (4)	−0.4361 (4)	0.0355
O(7)	−0.0316 (8)	−0.4155 (4)	−0.1694 (5)	0.0432
O(8)	0.2406 (8)	−0.4843 (4)	−0.0892 (5)	0.0443
O(9)	−0.0010 (9)	−0.4220 (5)	0.0321 (5)	0.0498
O(10)	0.540 (1)	0.1040 (7)	−0.2762 (9)	0.1031
O(11)	−0.532 (3)	0.044 (2)	−0.476 (2)	0.1272
O(121)	−0.291 (2)	−0.421 (2)	−0.101 (2)	0.1029
O(122)	−0.282 (6)	−0.424 (2)	−0.159 (2)	0.1889

[a] $U_{eq} = {}^4/_3(8\pi^2)^{-1}\sum_i\sum_j\beta_{ij}\mathbf{a}_i\cdot\mathbf{a}_j$.

Table IV. Bond Distances (Å) Involving Non-Hydrogen Atoms in MnCu(Cl_4obbz)$(H_2O)_5$

Cu–O(3)	1.905 (5)	N(1)–C(1)	1.334 (8)
Cu–O(4)	1.937 (4)	N(1)–C(3)	1.413 (8)
Cu–N(1)	1.914 (5)	N(2)–C(2)	1.330 (9)
Cu–N(2)	1.919 (5)	N(2)–C(10)	1.415 (8)
Mn–O(6)	2.108 (5)	C(1)–C(2)	1.533 (9)
Mn–O(7)	2.144 (5)	C(3)–C(4)	1.392 (9)
Mn–O(8)	2.169 (4)	C(3)–C(8)	1.42 (1)
Mn–O(9)	2.154 (4)	C(4)–C(5)	1.362 (9)
Mn–O(10)	2.219 (6)	C(5)–C(6)	1.37 (1)
Mn–O(11)	2.219 (5)	C(6)–C(7)	1.364 (9)
Cl(1)–C(4)	1.733 (7)	C(7)–C(8)	1.390 (9)
Cl(2)–C(6)	1.733 (6)	C(8)–C(9)	1.493 (9)
Cl(3)–C(11)	1.733 (7)	C(10)–C(11)	1.384 (9)
Cl(4)–C(13)	1.744 (7)	C(10)–C(15)	1.392 (9)
O(1)–C(1)	1.233 (9)	C(11)–C(12)	1.384 (9)
O(2)–C(2)	1.242 (8)	C(12)–C(13)	1.37 (1)
O(3)–C(9)	1.287 (8)	C(13)–C(14)	1.37 (1)
O(4)–C(16)	1.286 (7)	C(14)–C(15)	1.394 (8)
O(5)–C(9)	1.241 (8)	C(15)–C(16)	1.49 (1)
O(6)–C(16)	1.230 (8)		

axial positions chlorine atoms from neighboring molecules are found at rather long distances with Cu···Cl(2)($x - {}^1/_2$, ${}^1/_2 - y$, ${}^1/_2 + z$) = 2.930 Å and Cu···Cl(4)(${}^1/_2 + x$, ${}^1/_2 - y$, $z - {}^1/_2$) = 3.422 Å. These interactions link molecules related by the n-glide symmetry operation into chains, as shown in Figure 2. The dihedral angle between the best equatorial least-squares planes of Mn and Cu atoms is 23.8°. The bridging carboxylate group makes angles of 6.0 and 29.8° with the equatorial planes of manganese and copper atoms, respectively. The considerable difference in these two angles may be rationalized by considering the effects of the intramolecular hydrogen bond O(8)–H(81)···O(4) of 2.705 (7) Å. Due to steric hindrance between the ortho-substituted chlorine atoms and oxygen atoms (Cl(1)···O(1) = 2.948 (4) Å, Cl(3)···O(2) = 2.983 (5) Å), the oxamide group is bent out of the copper equatorial plane, the dihedral angle being 34.8°.

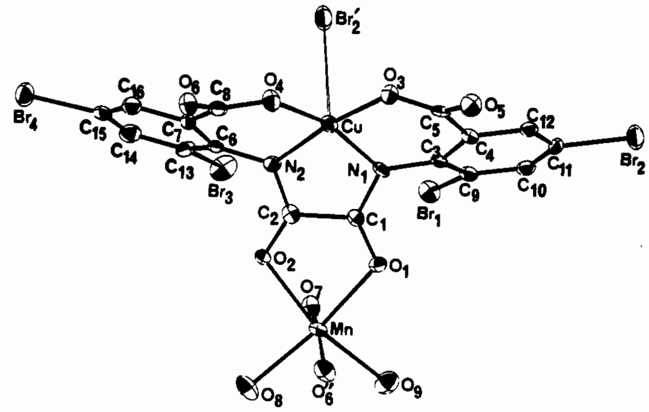

Figure 3. View of the MnCu(Br_4obbz)$(H_2O)_3$ unit with atomic numbering scheme. This view also shows the semicoordinating bromine atom belonging to a neighboring chain and an oxygen atom bound to the manganese(II) ion and belonging to a neighboring unit along the same chain.

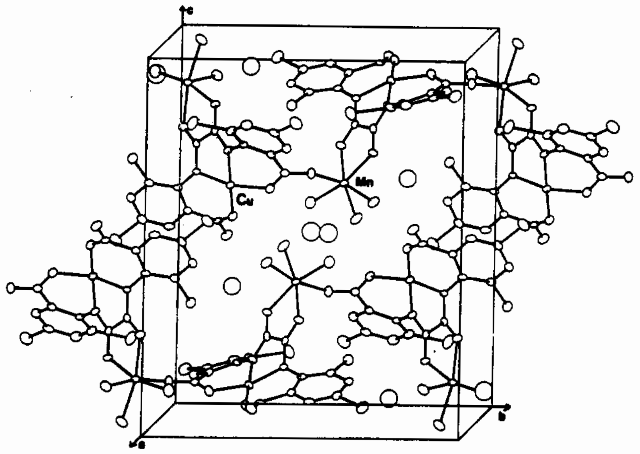

Figure 4. Packing view of the unit cell content for MnCu(Br_4obbz)$(H_2O)_3\cdot2.5H_2O$.

The Mn···Cu separation within the binuclear unit is 5.195 (1) Å. The shortest intermolecular metal···metal distance occurs between Mn atoms related by an inversion center, with Mn···Mn^i = 5.376 (1) Å, the exponent i standing for the position ($1 - x$, $-y$, $1 - z$); the two atoms are connected through hydrogen bonds between water molecules of their coordination spheres, O(8)–H(82)···O(11)^i = 2.880 Å. The Mn···Cu distance between molecules related by the same inversion center is 5.801 (1) Å, and Cu and Mn coordination spheres are also connected through hydrogen bonds, with O(3)···H(71)–O(7)^i = 2.775 (7) Å. Cu···Cu intermolecular separations are longer, the shortest one occurring between n-glide related molecules, with Cu···Cu($-{}^1/_2 + x$, ${}^1/_2 + y$, $-{}^1/_2 + z$) = 7.101 (1) Å.

The packing of the molecules within the crystal lattice is illustrated in Figure S1. The molecules are connected through an extensive network of hydrogen bonds; a complete list is given in Table SVI. In addition, there are Cu···Cl links as mentioned above.

MnCu(Br_4obbz)$(H_2O)_3\cdot2.5H_2O$. Bond lengths and angles involving all atoms but hydrogens are given in Tables VI and VII. Figure 3 shows the MnCu(Br_4obbz)$(H_2O)_3$ unit and Figure 4 a packing view emphasizing the chain structure. The structure consists of Mn(II)–Cu(II) alternating bimetallic chains running along the c axis of the monoclinic lattice, and noncoordinated water molecules. Along the chain, each MnCu(Br_4obbz)$(H_2O)_3$ unit is deduced from its neighbor by the glide plane so that the Mn–Cu vector which is nearly perpendicular to that glide plane is alternatively up and down as schematized below:

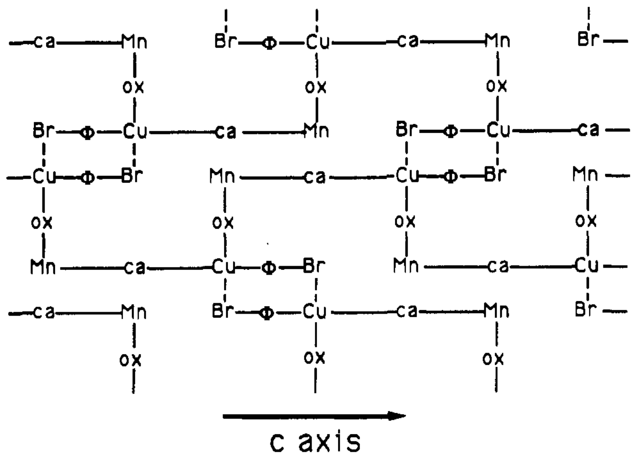

ox and ca stand for oxamide and carboxylate bridges, respectively. Φ denotes the aromatic ring and Br the bromine substituent in the 5-position. Cu···Br denotes the semicoordinative contact between bromine and copper atoms (see below).

The copper atom is bound to carboxylate oxygen atoms O(3) and O(4), and to both oxamide nitrogen atoms N(1) and N(2). These four atoms define a least-squares plane, called hereafter the copper basal plane, with 0.084 Å as the largest deviation. The inversion center transforms a chain into another parallel one. Chains are connected by semicoordinative Cu–Br bonds set up between copper and bromine Br(2) of a first chain and symmetrically related copper and bromine atoms of the second chain, as shown in Figures 4 and 5. As a result, the copper atom is located at 0.216 Å above the basal plane of a square pyramid, the apex of which is occupied by the bromine atom. The Cu–Br distance is 2.971 Å.

The manganese atom is octahedrally surrounded by six oxygen atoms. It is bound to three facial water molecules, the two oxamide oxygen atoms and one carboxylate oxygen atom of a neighboring unit. Thus, the two carboxylate groups of a ligand Br_4obbz^{4-} are not similar; one is bound to one copper atom while the other one bridges copper and manganese atoms in an anti–syn configuration.

The plane O(1), O(2), O(8), and O(9) made of both oxamide oxygen atoms and the two oxygen atoms trans to them with respect to Mn hereafter is called the manganese basal plane. If so defined, the copper and manganese basal planes are far from being coplanar. The dihedral angle between them is equal to 34.8°. This important bending may be understood as follows: the bromine atom Br(1) is in the ortho position with respect to the oxamide nitrogen atom N(1). It follows that atoms Br(1), C(9), C(3), N(1), C(1), and O(1) form a ring, and similarly for Br(3), C(13), C(6), N(2), C(2), O(2). A strong steric hindrance arises between Br and O atoms. If they were in the same plane, the Br–O distance would be 1.52 Å, using interatomic distances deduced from the X-ray analysis. The Br(1)–O(1) distance actually is equal to 3.088 Å because of this 34.8° dihedral angle, which releases the steric hindrance. To get this result, a rotation of the plane O(1), C(1), N(1), O(2), C(2), N(2) occurs around the N(1)–N(2) direction (see Figure 5), and the dihedral angle between this plane and the copper basal plane is 37.6°. It may be noticed that the aromatic ring with its bromine substituents, the oxamide nitrogen, and the carboxylate carbon atoms are nearly in the same least-squares plane, the largest deviation being 0.169 Å for Br(1) (or Br(3)). Without bromine on the aromatic ring, there is no need for such a large bending, and a smaller angle is enough to avoid the hindrance, as observed for $MnCu(obp)(H_2O)_3{\cdot}H_2O$ and $MnCu(obzp)(H_2O)_3{\cdot}H_2O$. As a matter of fact, the dihedral angles between the copper and manganese basal planes for these two compounds are equal to 15.6° and 10.3°, respectively.[17,18]

Table V. Bond Angles (deg) Involving Non-Hydrogen Atoms in $MnCu(Cl_4obbz)(H_2O)_5$

O(3)–Cu–O(4)	86.8 (2)	N(2)–C(2)–C(1)	113.8 (5)
O(3)–Cu–N(1)	94.6 (2)	N(1)–C(3)–C(4)	122.8 (6)
O(3)–Cu–N(2)	175.6 (2)	N(1)–C(3)–C(8)	120.3 (6)
O(4)–Cu–N(1)	163.5 (2)	C(4)–C(3)–C(8)	116.9 (5)
O(4)–Cu–N(2)	92.2 (2)	Cl(4)–C(4)–C(3)	119.9 (5)
N(1)–Cu–N(2)	85.2 (2)	Cl(1)–C(4)–C(5)	117.5 (5)
O(6)–Mn–O(7)	171.6 (2)	C(3)–C(4)–C(5)	122.4 (7)
O(6)–Mn–O(8)	91.6 (2)	C(4)–C(5)–C(6)	119.5 (6)
O(6)–Mn–O(9)	95.3 (2)	Cl(2)–C(6)–C(5)	120.2 (5)
O(6)–Mn–O(10)	98.3 (2)	Cl(2)–C(6)–C(7)	119.7 (5)
O(6)–Mn–O(11)	84.8 (2)	C(5)–C(6)–C(7)	120.0 (6)
O(7)–Mn–O(8)	87.3 (2)	C(6)–C(7)–C(8)	121.3 (6)
O(7)–Mn–O(9)	87.4 (2)	C(3)–C(8)–C(7)	118.8 (6)
O(7)–Mn–O(10)	89.9 (2)	C(3)–C(8)–C(9)	125.2 (5)
O(7)–Mn–O(11)	87.1 (2)	C(7)–C(8)–C(9)	115.5 (6)
O(8)–Mn–O(9)	167.3 (2)	O(3)–C(9)–O(5)	119.6 (6)
O(8)–Mn–O(10)	84.2 (2)	O(3)–C(9)–C(8)	121.7 (6)
O(8)–Mn–O(11)	98.0 (2)	O(5)–C(9)–C(8)	118.6 (6)
O(9)–Mn–O(10)	84.3 (2)	N(2)–C(10)–C(11)	121.9 (6)
O(9)–Mn–O(11)	93.3 (2)	N(2)–C(10)–C(15)	120.3 (6)
O(10)–Mn–O(11)	176.2 (2)	C(11)–C(10)–C(15)	117.7 (6)
Cu–O(3)–C(9)	128.9 (4)	Cl(3)–C(11)–C(10)	121.0 (5)
Cu–O(4)–C(16)	128.2 (4)	Cl(3)–C(11)–C(12)	116.7 (5)
Mn–O(6)–C(16)	133.0 (4)	C(10)–C(11)–C(12)	122.1 (6)
Cu–N(1)–C(1)	109.6 (4)	C(11)–C(12)–C(13)	118.3 (6)
Cu–N(1)–C(3)	125.3 (4)	Cl(4)–C(13)–C(12)	119.0 (5)
C(1)–N(1)–C(3)	121.5 (6)	Cl(4)–C(13)–C(14)	118.9 (5)
Cu–N(2)–C(2)	109.8 (4)	C(12)–C(13)–C(14)	122.1 (6)
Cu–N(2)–C(10)	124.7 (4)	C(13)–C(14)–C(15)	118.9 (6)
C(2)–N(2)–C(10)	122.6 (5)	C(10)–C(15)–C(14)	120.7 (6)
O(1)–C(1)–N(1)	129.0 (6)	C(10)–C(15)–C(16)	124.7 (5)
O(1)–C(1)–C(2)	117.9 (6)	C(14)–C(15)–C(16)	114.6 (6)
N(1)–C(1)–C(2)	113.1 (6)	O(4)–C(16)–O(6)	122.3 (6)
O(2)–C(2)–N(2)	127.1 (6)	O(4)–C(16)–C(15)	118.9 (6)
O(2)–C(2)–C(1)	119.1 (6)	O(6)–C(16)–C(15)	118.7 (5)

Table VI. Bond Distances (Å) Involving Non-Hydrogen Atoms in $MnCu(Br_4obbz)(H_2O)_3{\cdot}2.5H_2O$

Cu(1)–N(1)	1.922 (7)	C(3)–C(4)	1.40 (1)
Cu(1)–N(2)	1.933 (7)	C(3)–C(9)	1.40 (1)
Cu(1)–O(3)	1.921 (6)	C(3)–N(1)	1.39 (1)
Cu(1)–O(4)	1.957 (6)	C(4)–C(5)	1.52 (1)
Cu(1)–Br(2)[a]	2.971 (2)	C(4)–C(12)	1.41 (1)
Mn(1)–O(1)	2.161 (6)	C(5)–O(3)	1.28 (1)
Mn(1)–O(2)	2.204 (6)	C(5)–O(5)	1.24 (1)
Mn(1)–O(6)	2.178 (6)	C(6)–C(7)	1.41 (1)
Mn(1)–O(7)	2.178 (7)	C(6)–C(13)	1.41 (1)
Mn(1)–O(8)	2.173 (7)	C(6)–N(2)	1.40 (1)
Mn(1)–O(9)	2.159 (8)	C(7)–C(8)	1.49 (1)
Br(1)–C(9)	1.89 (1)	C(7)–C(16)	1.38 (1)
Br(2)–C(11)	1.897 (9)	C(8)–O(4)	1.28 (1)
Br(3)–C(13)	1.887 (9)	C(8)–O(6)	1.25 (1)
Br(4)–C(15)	1.88 (1)	C(9)–C(10)	1.36 (1)
C(1)–C(2)	1.53 (1)	C(10)–C(11)	1.41 (1)
C(1)–N(1)	1.33 (1)	C(11)–C(12)	1.36 (1)
C(1)–O(1)	1.25 (1)	C(13)–C(14)	1.36 (1)
C(2)–N(2)	1.32 (1)	C(14)–C(15)	1.36 (1)
C(2)–O(2)	1.25 (1)	C(15)–C(16)	1.38 (1)

[a] Refers to atom deduced by inversion center.

The Mn···Cu intrachain separations are equal to 5.341 (2) Å through the oxamide bridge, and 5.394 (2) Å through the carboxylate bridge. Another short Mn···Mn separation, 5.432 (3) Å, occurs between two manganese atoms related by inversion.

Parallel chains are not only connected by Cu–Br semicoordinative bonds but also by hydrogen bonds, of which a list is given in Table SVI. Two water molecules linked to manganese are bound to both oxygen atoms of the same carboxylate group. Thus O(3) is bound to O(7′) with a O(3)–O(7′) distance of 2.810 Å and an angle O(3)–H(71′)–O(7′) of 168 (10)°. O(5) is bound to O(8′) with a distance O(5)–O(8′) of 2.724 (10) Å and an angle O(3)–H(81′)–O(8′) of 154 (10)°. The prime notes the atoms of an adjacent chain deduced from the atoms listed in Table IV by the screw axis.

---

(17) Pei, Y.; Kahn, O.; Sletten, J.; Renard, J. P.; Georges, R.; Gianduzzo, J. C.; Curely, J.; Xu, Q. *Inorg. Chem.* **1988**, *27*, 47.

(18) Pei, Y.; Nakatani, K.; Kahn, O.; Sletten, J.; Renard, J. P. *Inorg. Chem.* **1989**, *28*, 3170.

Table VII. Bond Angles (deg) Involving Non-Hydrogen Atoms in MnCu(Br_4obbz)$(H_2O)_3 \cdot 2.5H_2O$

N(2)–Cu(1)–N(1)	83.8 (3)	N(2)–C(6)–C(7)	120.6 (8)
O(3)–Cu(1)–N(1)	91.8 (3)	N(2)–C(6)–C(13)	122.4 (8)
O(4)–Cu(1)–N(2)	89.7 (3)	C(8)–C(7)–C(6)	122.2 (8)
O(4)–Cu(1)–O(3)	92.3 (3)	C(16)–C(7)–C(6)	120.5 (9)
N(1)–Cu(1)–Br(2)[a]	101.1 (2)	C(16)–C(7)–C(8)	117.3 (8)
N(2)–Cu(1)–Br(2)[a]	94.3 (2)	O(4)–C(8)–C(7)	121.2 (8)
O(3)–Cu(1)–Br(2)[a]	93.9 (2)	O(6)–C(8)–C(7)	117.5 (8)
O(4)–Cu(1)–Br(2)[a]	96.4 (2)	O(6)–C(8)–O(4)	121.3 (9)
O(2)–Mn(1)–O(1)	76.9 (2)	C(3)–C(9)–Br(1)	121.0 (7)
O(6)–Mn(1)–O(1)	98.9 (3)	C(10)–C(9)–Br(1)	116.3 (7)
O(6)–Mn(1)–O(2)	90.1 (2)	C(10)–C(9)–C(3)	122.3 (9)
O(7)–Mn(1)–O(1)	90.8 (3)	C(11)–C(10)–C(9)	118.2 (9)
O(7)–Mn(1)–O(2)	100.1 (3)	C(10)–C(11)–Br(2)	117.5 (7)
O(8)–Mn(1)–O(2)	93.5 (3)	C(12)–C(11)–Br(2)	120.7 (7)
O(8)–Mn(1)–O(6)	88.9 (3)	C(12)–C(11)–C(10)	121.6 (9)
O(8)–Mn(1)–O(7)	83.1 (3)	C(11)–C(12)–C(4)	119.4 (9)
O(9)–Mn(1)–O(1)	90.3 (3)	C(6)–C(13)–Br(3)	119.7 (7)
O(9)–Mn(1)–O(6)	84.6 (3)	C(14)–C(13)–Br(3)	118.5 (8)
O(9)–Mn(1)–O(7)	87.3 (3)	C(14)–C(13)–C(6)	121.6 (9)
O(9)–Mn(1)–O(8)	100.2 (3)	C(15)–C(14)–C(13)	120.3 (10)
N(1)–C(1)–C(2)	113.3 (8)	C(14)–C(15)–Br(14)	119.8 (8)
O(1)–C(1)–C(2)	117.8 (8)	C(16)–C(15)–Br(4)	120.1 (8)
O(1)–C(1)–N(1)	128.9 (9)	C(16)–C(15)–C(14)	120.1 (9)
N(2)–C(2)–C(1)	113.0 (8)	C(15)–C(16)–C(7)	120.2 (9)
O(2)–C(2)–C(1)	118.5 (8)	C(1)–N(1)–Cu(1)	109.4 (6)
O(2)–C(2)–N(2)	128.5 (8)	C(3)–N(1)–Cu(1)	126.5 (6)
C(9)–C(3)–C(4)	117.8 (8)	C(3)–N(1)–C(1)	122.5 (8)
N(1)–C(3)–C(4)	120.0 (8)	C(2)–N(2)–Cu(1)	110.2 (6)
N(1)–C(3)–C(9)	122.1 (8)	C(6)–N(2)–Cu(1)	124.0 (6)
C(5)–C(4)–C(3)	123.2 (8)	C(6)–N(2)–C(2)	124.7 (8)
C(12)–C(4)–C(3)	120.2 (8)	C(1)–O(1)–Mn(1)	114.3 (6)
C(12)–C(4)–C(5)	116.5 (8)	C(2)–O(2)–Mn(1)	112.3 (6)
O(3)–C(5)–C(4)	120.3 (8)	C(5)–O(3)–Cu(1)	128.0 (6)
O(5)–C(5)–C(4)	117.9 (8)	C(8)–O(4)–Cu(1)	129.3 (6)
O(5)–C(5)–O(3)	121.7 (8)	C(8)–O(6)–Mn(1)	137.2 (6)
C(13)–C(6)–C(7)	116.9 (8)		

[a] Refers to atom deduced by inversion center.

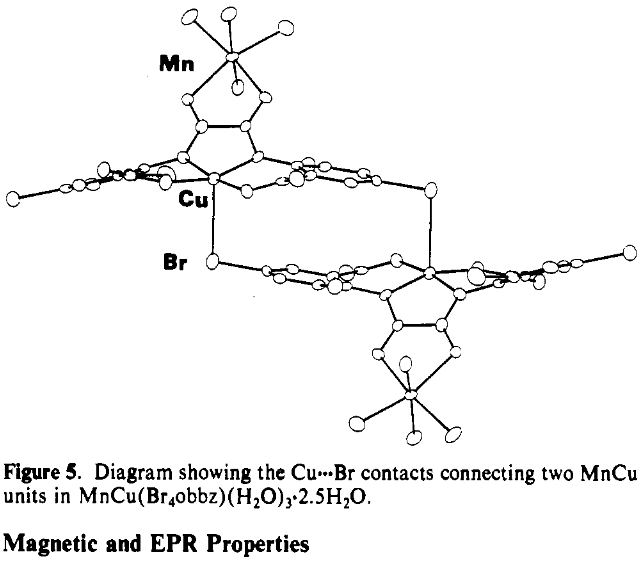

Figure 5. Diagram showing the Cu···Br contacts connecting two MnCu units in MnCu(Br_4obbz)$(H_2O)_3 \cdot 2.5H_2O$.

Magnetic and EPR Properties

MnCu(Cl_4obbz)$(H_2O)_5$. From 300 down to 2 K, the magnetic susceptibility of MnCu(Cl_4obbz)$(H_2O)_5$ perfectly follows a Curie law with $\chi_M T = 4.80$ cm^3 K mol^{-1}. This value exactly corresponds to what is expected for uncoupled Mn(II) and Cu(II) ions [$\chi_M T = (N\beta^2/12k)(35g_{Mn}^2 + 3g_{Cu}^2)$]. Therefore, the interaction through the carboxylato bridge is so small that it cannot be detected through magnetic measurements.

The X-band EPR spectrum shows a single and rather symmetrical resonance centered at $g = 2.045$ (5). The line width is equal to 630 G at 140 K and does not vary significantly with temperature. This spectrum indicates that the Mn(II) and Cu(II) ions are not rigorously magnetically isolated since it does not consist of the superposition of single-ion spectra. Once again, EPR provides information on the interaction between the magnetic centers that is not detectable through magnetic susceptibility measurements.[19]

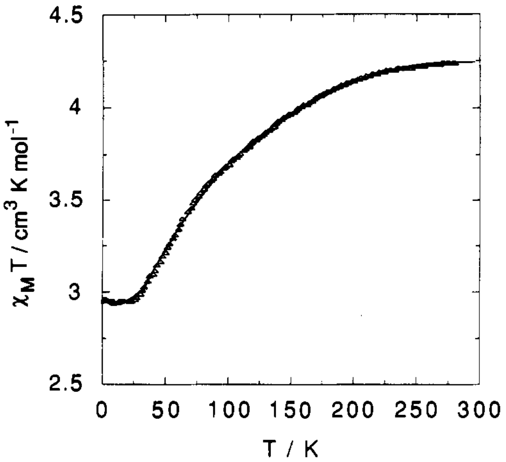

Figure 6. Experimental and calculated $\chi_M T$ versus T plots for MnCu(Br_4obbz)$(H_2O)_3 \cdot 2.5H_2O$.

MnCu(Br_4obbz)$(H_2O)_3 \cdot 2.5H_2O$. The magnetic behavior of this compound is shown in Figure 6 in the form of the $\chi_M T$ versus T plot. At room temperature, $\chi_M T$ is equal to 4.27 cm^3 K mol^{-1}, which is slightly below what is expected for isolated Mn(II) and Cu(II) ions. When the temperature is lowered, $\chi_M T$ continuously decreases and reaches a plateau around 20 K with $\chi_M T = 2.95$ cm^3 K mol^{-1}. $\chi_M T$ is then constant down to 2 K. Those magnetic data closely follow eq 1, which is valid for an isolated Mn(II)–Cu(II) pair with an antiferromagnetic intrachain interaction. The symbols N, β, and k have their usual meaning. J is the interaction parameter occurring in the spin Hamiltonian $-JS_{Mn} \cdot S_{Cu}$, and g_2 and g_3 are the Zeeman factors associated with the $S = 2$ and 3 pair states, respectively, arising from the interaction between the local $S_{Mn} = {}^5/_2$ and $S_{Cu} = {}^1/_2$ states. The plateau below 20 K corresponds to the temperature range where only the ground $S = 2$ pair state is thermally populated. The least-squares fitting of the experimental data with eq 1 leads to $J = -29.0$ cm^{-1}, $g_2 = 1.97$, and $g_3 = 1.99$. The agreement factor defined by $\sum[(\chi_M T)^{obs} - (\chi_M T)^{calc}]^2/\sum[(\chi_M T)^{obs}]^2$ is then equal to 1.2×10^{-5}. The energy gap between quintet and septet pair states is equal to $3J = -87$ cm^{-1}. g_2 and g_3 in principle may be related to the local Zeeman factors g_{Mn} and g_{Cu} through[8,20,21]

$$\chi_M T = (2N\beta^2/k)[5g_2^2 + 14g_3^2 \exp(3J/kT)]/[5 + 7\exp(3J/kT)] \quad (1)$$

$$g_2 = (7g_{Mn} - g_{Cu})/6$$
$$g_3 = (5g_{Mn} + g_{Cu})/6 \quad (2)$$

g_{Mn} and g_{Cu} deduced from eq 2 are found equal to 1.97 and 2.04, respectively.

The X-band EPR spectrum shows a single resonance centered at $g = 2.03$. The line width is equal to 480 G at 140 K and is almost independent of the temperature. This spectrum does not correspond to magnetically isolated Mn(II)–Cu(II) pairs. If so, it would present four lines at low temperature due to the zero-field splitting within the $S = 2$ ground state.[22,23] Again, EPR reveals long-range interactions not detectable through magnetic susceptibility measurements.[24,25]

---

(19) Journaux, Y.; Kahn, O.; Morgenstern-Badarau, I.; Galy, J.; Jaud, J.; Bencini, A.; Gatteschi, D. *J. Am. Chem. Soc.* **1985**, *107*, 6305.

(20) Scaringe, R. P.; Hodgson, D.; Hatfield, W. E. *Mol. Phys.* **1978**, *35*, 701.

(21) Gatteschi, D.; Bencini, A. In *Magneto-Structural Correlations in Exchange Coupled Systems*; Willett, R. D., Gatteschi, D., Kahn, O. Eds.; D. Reidel: Dordrecht, The Netherlands, 1983; p 242.

(22) Krost, D. A.; McPherson, G. L. *J. Am. Chem. Soc.* **1978**, *100*, 987.

(23) Paulson, J. A.; Krost, D. A.; McPherson, G. L.; Rogers, R. D.; Atwood, J. L. *Inorg. Chem.* **1980**, *19*, 2519.

(24) Gatteschi, D.; Guillou, O.; Zanchini, C.; Sessoli, R.; Kahn, O.; Verdaguer, M.; Pei, Y. *Inorg. Chem.* **1989**, *28*, 287.

(25) Gatteschi, D.; Zanchini, C.; Kahn, O.; Pei, Y. *Chem. Phys. Lett.* **1989**, *160*, 157.

Discussion

In the last section, we would like first to compare the structures of the two title compounds **1** and **2**, then to compare the structure of **2** with those of the bimetallic alternating chains previously described, and finally to discuss the magnetic properties of the tetrachloro and tetrabromo derivatives and to extract the information of interest for this class of Mn(II)–Cu(II) systems.

The first problem we face when comparing the structures of the two title compounds is to explain why the oxamide group binds the Mn(II) ion in **2** while it does not in **1**. Actually, two rationalizations of this quite unexpected result can be proposed. (i) There is a competition between the tendency of the oxamide group to bind a metal center through its oxygen atoms and the steric hindrance due to the halogeno substituent in the 3-position on the aromatic ring. The chlorine substituent has a stronger electron-withdrawing power, which diminishes the coordinating ability of the oxamide oxygen atoms, and the steric effect dominates. The large dihedral angles between the oxamide plane and copper basal plane (34.8 and 36.7° in the chloro and bromo derivatives, respectively) caused by the repulsion between halogen substituents in the 3-position and oxamide oxygen atoms, imposes a pronounced bending of the Mn–oxamide–Cu network in the chain structure. On the other hand, the bromine substituent has a less electron-withdrawing power, so that the coordinating ability of the oxamide oxygen atoms dominates, which imposes a pronounced bending of the Mn–oxamide–Cu network. This is allowed through electron delocalization occurring all along the C(9)–C(3)–N(1)–C(1)–O(1) linkage as shown by interatomic distances of 1.40, 1.39, 1.33, and 1.25 Å, successively. (ii) The change of coordination around the manganese atom is due to the difference in steric bulk between chlorine and bromine, which in turn leads to the change in coordination ability of the oxamido oxygen atoms. Such an argument is substantiated when comparing the dihedral angles between the least-squares plane N1–C1–N2–C2 (plane A) and those of the aromatic rings (planes B and C). Dihedral angles between A and B are equal to 45.0 and 52.0°, and between A and C to 53.0 and 58.6° for **1** and **2**, respectively. It follows that the oxamide nitrogen atoms are more conjugated to the electron-deficient phenyl rings in **1** than in **2**. Loss of electron density from the amide nitrogen atoms to the aromatic rings occurs at the direct expense of electron density at the amide oxygen atoms through a resonance mechanism. It is certainly difficult to choose between explanations i and ii. We would say that the two effects might be operative.

The structures of two alternating chain compounds have already been described, namely MnCu(obp)[17] and MnCu(obzp)[18] with obp = oxamidobis(*N*,*N'*-propionato) and obzp = oxamido-*N*-benzoato-*N'*-propionato. For the sake of simplicity, we will ignore the water molecules involved in the formulas. For both compounds as well as for **2**, the Mn(II) and Cu(II) ions are alternately bridged by oxamide and carboxylate groups. The Mn···Cu distances through the oxamide bridge are rather similar for the obp and the obzp derivatives (5.452 (2) and 5.4376 (4) Å, respectively), but this distance is significantly shorter for the Br$_4$obbz derivative (5.341 (2) Å). This difference is obviously due to the more pronounced bending of the Mn–oxamide–Cu network in **2**. The dihedral angle between the manganese and copper basal planes is equal to 34.8° in this compound and to 15.6° and 10.3° in MnCu(obp) and MnCu(obzp), respectively. As for the Mn···Cu separations through the carboxylate group, they are rather similar in MnCu(obzp) and **2** (5.3670 (4) and 5.394 (2) Å, respectively), but the separation is much larger in MnCu(obp). This difference reflects the anti–syn configuration of the carboxylate bridge for the first two compounds, and the anti–anti configuration for the third one, as schematized below:

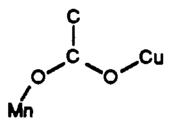

anti–syn

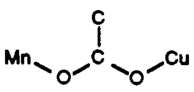

anti–anti

We will see later the consequences of these structural differences on the magnetic properties. Owing to the Cu–Br interaction, the copper atom is more pushed out of its basal plane in **2** (0.216 Å) than in the other two compounds (0.114 Å in MnCu(obp), where an oxygen atom of an adjacent chain occupies an apical position, and 0.022 Å in MnCu(obzp)). Another difference deserving to be mentioned is that the three water molecules linked to the manganese atom in **2** are facial while they are meridional in MnCu(obp) and MnCu(obzp).

To finish this structural discussion, we would like to point out that the coordination of the carboxylate bridge is anti–syn for both title compounds. The Mn···Cu separation is however shorter in the tetrachloro derivative than in the tetrabromo (5.195 (2) and 5.394 (2) Å, respectively). This is in part caused by the shorter Mn–O(6) distance and smaller Mn–O(6)–C angle in the tetrachloro derivative (2.108 Å and 133.0° as compared to 2.176 Å and 137.2° in the tetrabromo derivative) and in part by the differences in planarity of the Mn–carboxylate–Cu network. In the tetrachloro derivative, the Mn atom is deviating only slightly (−0.034 Å) from the carboxylate plane, and the Cu atom, deviating by 0.691 Å from this plane, is slightly closer to Mn than it would have been if coplanar. In the tetrabromo derivative, the Cu atom deviates slightly less from the carboxylate plane (0.462 Å), but here the Mn atom is twisted out of the plane by 0.645 Å, causing a larger Mn···Cu separation across the carboxylate bridge in the anti–syn configuration.

1 has the structure of a Mn(II)–Cu(II) binuclear compound, and **2**, that of a Mn(II)–Cu(II) alternating chain. However, the former derivative shows the magnetic behavior of isolated Mn(II) and Cu(II) ions, and the latter, that of isolated Mn(II)–Cu(II) pairs. This is due to the fact that in both compounds the interaction between the Mn(II) and Cu(II) ions through the carboxylate bridge is negligible owing to the anti–syn configuration of this bridge. In contrast, for MnCu(obp), the configuration of the carboxylate bridge is anti–anti and the interaction between Mn(II) and Cu(II) ions through this group is characterized by $J = -6.8$ (7) cm^{-1}. MnCu(obp) magnetically behaves as a ferrimagnetic chain compound with the characteristic minimum in the $\chi_M T$ versus T plot.[17] In a previous paper, we explained why the magnetic orbitals centered on Mn(II) and Cu(II) ions were favorably oriented to interact in the anti–anti configuration and unfavorably oriented in the anti–syn configuration.[18] It is interesting to point out here that the anti–anti configuration leads to a much larger Mn···Cu separation. This confirms, if it was still necessary, that the distance between the magnetic centers is in no way a determinant factor as for the magnitude of the interaction. It seems that the anti–anti configuration around the carboxylate bridge is a prerequisite for observing the one-dimensional ferrimagnetic behavior in a Mn(II)–Cu(II) alternating chain compound involving copper precursors like

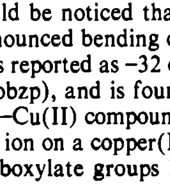

The strong interaction between Mn(II) and Cu(II) ions through the oxamido bridge in the tetrabromo derivative confirms the remarkable ability of conjugated bisbidentate ligands to transmit the electronic effects between magnetic centers rather apart from each other.[26] It should be noticed that the interaction is not diminished by the pronounced bending of the Mn–oxamide–Cu network. Indeed, J was reported as −32 cm^{-1} in MnCu(obp) and −27.4 cm^{-1} in MnCu(obzp), and is found as −29 cm^{-1} in **2**.

To date, five Mn(II)–Cu(II) compounds obtained through the reaction of the Mn(II) ion on a copper(II) precursor containing both oxamide and carboxylate groups have been investigated. These compounds present quite a surprising diversity as for their

---

(26) Kahn, O, *Angew. Chem., Int. Ed. Engl.* **1985**, *24*, 834.

crystal structures and their magnetic properties. Structural factors leading to one-dimensional ferrimagnetic behavior on the one hand and to interchain ferromagnetic interaction on the other hand are better and better understood. The control of these structural factors during the synthetic process remains however a very difficult task. The crystal engineering in molecular chemistry still is in its infancy.

Acknowledgment. We would like to express our deepest gratitude to the Société Nationale Elf Aquitaine which has financially supported this work and offered a research grant to K.N. We are also grateful to J. P. Renard for his help with the low-field SQUID magnetic measurements.

Supplementary Material Available: Tables SI-SIX, listing data collection and refinement information, anisotropic thermal parameters for the non-hydrogen atoms, coordinates for the hydrogen atoms, the hydrogen bond data, and the least-squares mean planes for both MnCu(Cl_4obbz)$(H_2O)_5$ and MnCu(Br_4obbz)$(H_2O)_3$·$2.5H_2O$, and Figure S1, showing a stereoview of packing of molecules within the crystal lattice of MnCu(Cl_4obbz)$(H_2O)_5$ (15 pages); tables of calculated and observed structure factors for MnCu(Cl_4obbz)$(H_2O)_5$ and MnCu(Br_4obbz)$(H_2O)_3$·$2.5H_2O$ (27 pages). Ordering information is given on any current masthead page.

Contribution from the Department of Chemistry,
Texas A&M University, College Station, Texas 77843

Solid-State NMR Studies of Magneto-Structural Correlations in Anhydrous Copper(II) Carboxylates

Gordon C. Campbell,† Joseph H. Reibenspies, and James F. Haw*

Received January 17, 1990

Magneto-structural correlations are probed in a series of anhydrous copper(II) carboxylates via solid-state NMR spectroscopic techniques. Temperature-dependent ^{13}C cross-polarization magic-angle-spinning (CP/MAS) results are presented for copper(II) propionate ($Cu_2(C_2H_5CO_2)_4$), copper(II) isobutyrate ($Cu_2(C_3H_7CO_2)_4$), and copper(II) isovalerate ($Cu_2(C_4H_9CO_2)_4$). Observed contact shifts are related to magnetic information and used to calculate singlet-triplet energy level separations ($-2J$), diamagnetic chemical shifts (δ_{dia}), and electron-nucleus hyperfine coupling constants (A). As structural information is manifest in NMR signal multiplicity, this report also includes an X-ray crystal structure determination of $Cu_2(C_4H_9CO_2)_4$. The compound crystallized in the triclinic space group $P\bar{1}$ (No. 2), with a = 5.1910 (13) Å, b = 10.840 (2) Å, c = 11.063 (2) Å, α = 83.120 (15)°, β = 86.92 (2)°, γ = 85.60 (2)°, Z = 1, and V = 615.6 (2) Å^3. Full-matrix least-squares refinement on F^2 yielded the final R value of 0.0654 for 1571 unique observed reflections.

Introduction

Copper(II) carboxylates, $Cu_2(RCO_2)_4L_n$ with $n = 0$ or $n = 2$, have been the focus of research attention since the early part of the twentieth century.[1] Interest in the magneto-structural correlations[2] in these (and related) materials spans fields ranging from chemistry to biology and physics. Although once somewhat controversial, the mechanism of antiferromagnetic coupling between dimeric copper centers is now generally thought to involve the electronic orbitals of the bridging carboxylate ligands in what is termed the superexchange pathway.[3] Recently,[4] two of us reported the role that solid-state nuclear magnetic resonance (NMR) spectroscopy can play in the development of a better understanding of the properties of these compounds. We were able to quantitatively refine earlier qualitative reports[5] and gain new insights into the relationship between structure and magnetism in a representative copper(II) carboxylate.

Variable-temperature[6] (VT) ^{13}C cross-polarization magic-angle-spinning (CP/MAS) NMR spectroscopy[7] has, we feel, provided the most convincing experimental evidence yet reported for magnetic superexchange between metal centers in these solids. Paramagnetic contact shifts were observed for all ^{13}C resonances corresponding to sites along the carboxylate bridges in anhydrous copper(II) n-butyrate ($R = C_3H_7$, $n = 0$). In addition to being directly related to the presence of unpaired electron density at these nuclei,[8] the temperature dependence of the shifts allowed the determination of electron-nucleus hyperfine coupling constants (A), singlet-triplet energy level separations ($-2J$, from the spin Hamiltonian $H = -2JS_1 \cdot S_2$), and diamagnetic chemical shifts (δ_{dia}). Signs and relative magnitudes of A values were shown to be related to mechanisms of magnetic superexchange coupling and structurally significant in a sense completely analogous to the Karplus relationship,[9] which is well-known in solution-state NMR spectroscopy. The reliability of $-2J$ values determined via NMR techniques is in principle superior to that from corresponding bulk measurements due to the relative insensitivity of NMR spectra to the presence of small amounts of paramagnetic impurities. Potential complications could arise, however, from

Table I. Crystallographic Data for Anhydrous Copper(II) Isovalerate

mol formula $C_{20}H_{36}O_8Cu_2$	space group $P\bar{1}$
fw 531.6	T = 193 K
a = 5.1910 (13) Å	λ = 0.7107 Å
b = 10.840 (2) Å	ρ_{obsd} = 1.46 g cm^{-3}
c = 11.063 (2) Å	ρ_{calcd} = 1.434 g cm^{-3}
α = 83.120 (15)°	μ = 1.769 mm^{-1}
β = 86.92 (2)°	rel transm factors: 0.9714-0.9928
γ = 85.60 (2)°	$R(F_o^2)$ = 0.065
V = 615.6 (2) Å^3	$R_w(F_o^2)$ = 0.063
Z = 1	

---

* To whom correspondence should be addressed.

† Present address: Polymers Division, National Institute of Standards and Technology, Gaithersburg, MD 20899.

(1) Lifschitz, J.; Rosenbohm, E. *Z. Electrochim.* **1915**, *21*, 499.

(2) (a) Willett, R. D., Gatteschi, D., Kahn, O., Eds. *Magneto-Structural Correlations in Exchange Coupled Systems*; Reidel: Boston, MA, 1985. (b) Melnik, M. *Coord. Chem. Rev.* **1982**, *42*, 259. (c) Battaglia, L. P.; Corradi, B.; Menabue, L. *J. Chem. Soc., Dalton Trans.* **1986**, 1653.

(3) (a) Gerloch, M.; Harding, J. H. *Proc. R. Soc. London A* **1978**, *360*, 211. (b) Harcourt, R. D.; Martin, G. E. *J. Chem. Soc., Faraday Trans.* **1977**, *73*, 1. (c) Rao, V. M.; Menohar, H. *Inorg. Chim. Acta* **1979**, *34*, L213.

(4) Campbell, G. C.; Haw, J. F. *Inorg. Chem.* **1988**, *27*, 3706.

(5) (a) Haw, J. F. Presentation at the 28th Rocky Mountain Conference, Denver, CO, 1986. (b) Campbell, G. C. Presentation at the 28th Experimental NMR Conference, Asilomar, CA, 1987. (c) Campbell, G. C. Presentation at the 29th Rocky Mountain Conference, Denver, CO, 1987. (d) Walter, T. H.; Oldfield, E. *J. Chem. Soc., Chem. Commun.* **1987**, 646.

(6) (a) Lyerla, J. R.; Yannoni, C. S.; Fyfe, C. A. *Acc. Chem. Res.* **1982**, *15*, 208. (b) Haw, J. F.; Campbell, G. C.; Crosby, R. C. *Anal. Chem.* **1986**, *58*, 3172. (c) Haw, J. F. *Anal. Chem.* **1988**, *60*, 559A.

(7) (a) Yannoni, C. S. *Acc. Chem. Res.* **1982**, *15*, 201. (b) Maciel, G. E. *Science* **1984**, *226*, 282.

(8) McConnell, H. M.; Holm, C. H. *J. Chem. Phys.* **1957**, *27*, 314.

(9) (a) Karplus, M. *J. Chem. Phys.* **1959**, *30*, 11. (b) Karplus, M. *J. Am. Chem. Soc.* **1963**, *85*, 2870.

0020-1669/91/1330-0171$02.50/0 © 1991 American Chemical Society